A Mode-Based Approach for Channel Modeling in Underground Tunnels under the Impact of Vehicular Traffic Flow

Zhi Sun, *Student Member, IEEE,* and Ian F. Akyildiz, *Fellow, IEEE*

***Abstract*—In underground tunnels with vehicular traffic flow, wireless communications experience severe fading problems due to the signal reflections and diffractions on the tunnel walls and the mobile vehicles. Currently, most of the existing tunnel channel models can only characterize the signal propagation in empty tunnels. Existing investigations on the influence of the vehicles are all limited to experimental or numerical results. This paper provides a theoretical analysis of the wireless channel in tunnels with vehicular traffic flow. First, the effects of a single vehicle on the signal propagation in a tunnel are investigated. The analytical expressions of the *in-mode loss* and the *mode coupling* coefficients are provided using the uniform theory of diffraction (UTD), Poisson summation formula, and the saddle point method. Then the channel model in a tunnel with either deterministic or random vehicular traffic flow is provided according to the analysis on a single vehicle's effect. The predicted received power given by our theoretical model has a good match with the numerical simulation results. Our channel model shows that the signal propagation in tunnels with vehicular traffic flow is influenced by multiple factors, including the number, the size and position of the vehicles, the size and the curvature of the tunnel, the vehicular traffic load, and the vehicle velocity.**

***Index Terms*—Channel model, underground tunnel, vehicular traffic flow, multi-mode model.**

I. Introduction

WIRELESS communications experience severe fading problems in underground tunnels with vehicular traffic flow [1]. Due to the reflections of the electromagnetic (EM) waves on the tunnel walls, the multipath effects are complicated and unique compared to the terrestrial wireless channels [3]–[5]. Moreover, the tunnels in operation are filled with mobile vehicles with random size and positions. The reflections and the diffractions on the vehicles make the wireless channel in the tunnel even more complicated. To establish reliable and efficient wireless communications in underground tunnels, the analytical channel model that explicitly contains the dependence on the tunnel geometry, vehicular traffic information, and other communication parameters is needed.

The channel models for empty tunnels have been well analyzed in the literature. Currently there are mainly three techniques to model the wireless channel [5], [6]: the Geometrical Optical model (GO model) [7], [8], the Waveguide model [9], [10], and the Full Wave model [11]. The GO model and the Full Wave model are limited to numerical results and may create great computational burdens. The waveguide model provides analytical results but is only applicable for the far region of the transmitter in empty tunnels. In [3], [4], we have developed the Multimode model that gives analytical results for both the near region and the far region in an empty tunnel. However, the model cannot characterize the influence of vehicles. For curved tunnels, the additional attenuation coefficients caused by the tunnel curvature are given in [12].

However, for tunnels with vehicular traffic flow, current channel analyses are limited to either experiments [13], [14] or numerical methods (i.e., GO model [15]–[17] and Full Wave model [18]). These experimental and numerical solutions cannot provide an explicit description on the effect of multiple environmental or communication parameters. Moreover, the numerical solutions require a great amount of input data of detailed geometric information of the vehicular traffic flow, which are infeasible to acquire from the in-operation tunnels. To the best of our knowledge, there is no analytical channel model developed to characterize the signal propagation in tunnels with vehicular traffic flow so far.

In this paper, we develop a channel model to analytically characterize the signal propagation in underground tunnels with vehicular traffic flows. In particular, due to the reflections and the diffractions of the plain waves on the vehicle, each propagation mode may experience the *in-mode loss* and the *mode coupling*. The closed-form in-mode loss and mode coupling coefficients are developed by the uniform theory of diffraction (UTD) [19], Poisson sum formula [20] and the saddle point method [21]. The field at the receiver is the joint effects of all the vehicles between the transceivers and the tunnel itself. Based on the analysis in the deterministic scenario, the channel model for tunnels with random vehicular traffic flows is also developed according to the traffic flow theory [22]. The entries of the propagation matrix are proved to have the normal distribution. Moreover, the means and the variables of the normal distributions are analytically expressed. Our analytical models are validated by comparing the theoretical predictions with the numerical simulation results. Based on the new channel models, we present an in-depth analysis on the signal propagation in tunnels with vehicular traffic, which is influenced by multiple factors including the number, size and position of the vehicles, the size and the curvature of the

Manuscript received April 27, 2010; revised March 8 and June 5, 2011; accepted July 5, 2011. The associate editor coordinating the review of this paper and approving it for publication was F. Tufvesson.

The authors are with the Broadband Wireless Networking Laboratory, School of Electrical & Computer Engineering, Georgia Institute of Technology, Atlanta, GA, 30332, USA (e-mail: {zsun; ian}@ece.gatech.edu).

A much shorter version of this paper appeared in [2].

Digital Object Identifier 10.1109/TWC.2011.080611.100710

tunnel, the vehicular traffic load, and the vehicle velocity.

The remainder of this paper is organized as follows. In Section II, the Multimode model for empty tunnels is briefly overviewed. In Section III, the signal propagation around a single vehicle is analyzed. In Section IV, the channel model for tunnels with deterministic and random vehicular traffic flows are developed. Then, in Section V, the influence of the vehicular traffic flow on the signal propagation is analyzed by the new model. Finally, the paper is concluded in Section VI.

II. Signal Propagation in Empty Tunnels

In this section, the Multimode model for empty tunnels [3], [4] is briefly overviewed, which lays the foundation of the analysis on the signal propagation in tunnels with vehicular traffic flow. Specifically, the empty tunnel is modeled as an oversized waveguide with imperfectly lossy walls. Multiple waveguide modes with different eigenfunctions and attenuation coefficients are transmitting simultaneously in the tunnel. The tunnel cross section is treated as an equivalent rectangular with a width of $2a$ m and a height of $2b$ m. A Cartesian coordinate system is set with its origin located at the center of the rectangle tunnel. Let $\mathbf{N}_{mode}$ be the set of significant modes in the tunnel. $\mathbf{N}_{mode} = \{(m,n)\}$ and $|\mathbf{N}_{mode}| = N$. Since the mode's attenuation rate rises fast as the mode order increases, only a small number of modes are left after the signal propagates for a certain distance. The number of significant modes that need to be considered is determined by multiple parameters, including the size of the tunnel, the distance between the transceivers, and the operating frequency. In most cases, the received signal strength is convergent when the first 50 ($m+n<10$) modes are considered. The electric field $E^{RX}(x_r, y_r, z_r)$ at the position of the receiver can be obtained by summing up the field of all significant modes, which is given by

$$E^{RX}(x_r, y_r, z_r) = \sqrt{G_t G_r} \cdot \sum_{(m,n)\in \mathbf{N}_{mode}} E^{eign}_{mn,(x_r,y_r)} \cdot e^{-\Gamma_{mn} \cdot z_r} \cdot C^{TX}_{mn}, \quad (1)$$

where z_r is the distance between the transmitter and receiver; (x_r, y_r) is the coordinate of the receiver at the tunnel cross section; G_t and G_r are the TX and RX antenna gain, respectively; $E^{eign}_{mn,(x_r,y_r)}$ is the value of the eigenfunction of the mode EH_{mn} at the position of the receiver; $\Gamma_{mn} = \alpha_{mn} + j\beta_{mn}$ where α_{mn} is the attenuation coefficient of the mode EH_{mn} and βmn is the phase shift coefficient of EH_{mn}; C^{Tx}_{mn} is the intensity of the mode EH_{mn} excited by the transmitter. The detailed expression of $E^{eign}_{mn,(x,y)}$, α_{mn}, β_{mn}, and C^{Tx}_{mn} can be found in [3], [4]. If the tunnel is curved, the expressions of α_{mn} and β_{mn} should be modified according to [12].

III. Signal Propagation around a Single Vehicle

The propagation modes can travel along the tunnel without interference with each other if the tunnel is empty. Vehicles may cause additional propagation loss. Moreover, part of the energy of each mode may be coupled to the other modes due to the existence of the vehicles. In this section, we analyze the influence of a single vehicle on the mode propagation.

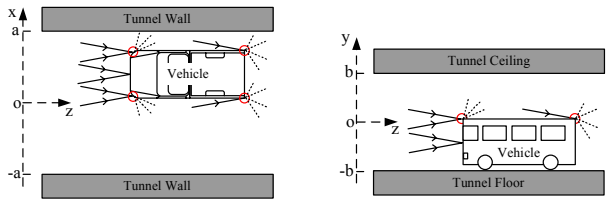

(a) Top view. In-mode loss due to the reflection on the vehicle's front surface. Mode coupling due to the diffraction on the four vertical edges around the vehicle.

(b) Side view. In-mode loss due to the reflection on the vehicle's front surface. Mode coupling due to the diffraction on the two horizontal edges on the top of the vehicle.

Fig. 1. Influence of a single vehicle on the mode propagation.

Without loss of generality, the vehicles are modeled as metal rectangular boxes with different sizes. According to US Federal Regulations, the width w, height h and length l of most vehicles (including cars, vans, buses and trucks) fall into the following intervals (unit is meter):

$$w \in [1.5, 2.5], \quad h \in [1.3, 4.2], \quad \text{and} \quad l \in [3.5, 16.2]. \quad (2)$$

A. Classification of Vehicle Influence

We assume that the TX antenna is a X-polarized electrical dipole. The results for Y-polarized antenna can be obtained in the similar way. The tunnel walls are made of concrete that have relative permittivity ε_w. The wave number k in the tunnel space is $k = 2\pi f\sqrt{\mu_0 \varepsilon_0}$, where μ_0 and ε_0 are the permeability and the permittivity of the air in the tunnel, respectively; and f is the operating frequency. Since the permittivity ε_w of the concrete tunnel wall is much larger than 1 and the wave number k is also large for high operating frequency (>1 GHz), the eigenfunction of X-polarized mode EH_{mn} provided by [3], [4], [10] can be simplified as

$$E^{eign}_{mn,(x,\ y)} \simeq \sin\left(\frac{m\pi}{2a}x + \varphi_x\right) \cdot \cos\left(\frac{n\pi}{2b}y + \varphi_y\right), \quad (3)$$

where $\varphi_x = 0$ if m is even; $\varphi_x = \frac{\pi}{2}$ if m is odd; $\varphi_y = 0$ if n is odd; $\varphi_y = \frac{\pi}{2}$ if n is even. It should be noted that we only consider the vehicle's influence on low order modes, since the power of the high order modes attenuates very fast.

Assuming that there is a vehicle with size $(w \times h \times l)$ inside the tunnel. Fig. 1 shows the top view and the side view of the tunnel with a vehicle. The vehicle is z_v meters apart from the transmitter. The middle axle of the vehicle lies parallel to the z-axes with the position $x = x_v$. In the empty tunnel between the transmitter and the vehicle, the field of EH_{mn} mode is:

$$E_{mn}(x,y,z) = C^{Tx}_{mn} \cdot e^{-\Gamma_{mn} \cdot z} \cdot E^{eign}_{mn,(x,y)}, \quad (4)$$

Substituting (3) into (4) yields:

$$\begin{aligned} &E_{mn}(x,y,z) \\ &\simeq C^{Tx}_{mn} \cdot e^{-\Gamma_{mn} \cdot z} \cdot \sin\left(\frac{m\pi}{2a}x + \varphi_x\right) \cdot \cos\left(\frac{n\pi}{2b}y + \varphi_y\right) \\ &= \frac{C^{Tx}_{mn} \cdot e^{-\alpha_{mn} \cdot z}}{4} \cdot \Big\{ \rho_1(m)\rho_2(n) e^{ik[\sin(\alpha_m)\cdot x + \sin(\beta_n)\cdot y - \beta_{mn}/k \cdot z]} \\ &\quad + \rho_2(m)\rho_2(n) e^{ik[\sin(-\alpha_m)\cdot x + \sin(\beta_n)\cdot y - \beta_{mn}/k \cdot z]} \\ &\quad + \rho_1(m)\rho_1(n) e^{ik[\sin(\alpha_m)\cdot x + \sin(-\beta_n)\cdot y - \beta_{mn}/k \cdot z]} \\ &\quad + \rho_2(m)\rho_1(n) e^{ik[\sin(-\alpha_m)\cdot x + \sin(-\beta_n)\cdot y - \beta_{mn}/k \cdot z]} \Big\}, \end{aligned} \quad (5)$$

where $\rho_1(u) = -j$ if u is even; $\rho_1(u) = 1$ if u is odd; $\rho_2(u) = j$ if u is even; $\rho_2(u) = 1$ if u is odd. It shows that each mode can be viewed as the superposition of four plane waves with four symmetric directions. $\pm\alpha_m$ and $\pm\beta_n$ are the grazing angles of the plane waves on the tunnel walls, and:

$$\sin(\alpha_m) = \frac{m\pi}{2ak} \quad \text{and} \quad \sin(\beta_n) = \frac{n\pi}{2bk}. \tag{6}$$

The higher order modes have larger grazing angles. Since higher order mode has much higher attenuation rate [3], [4], we focus on the lower order modes. For the lowest order mode EH_{11}, the grazing angle is very small (around 1°).

As illustrated in Fig. 1, the influence of the vehicle on the propagation mode EH_{mn} can be classified into two categories:

- The plane waves hitting the vehicle's front surface will be reflected back. Therefore, the energy of the waves hitting the vehicle's front surface can be viewed as an additional loss of the EH_{mn} mode caused by the vehicle. This type of influence is defined as *in-mode loss*.
- The plane waves hitting the edge between two surfaces of the vehicle will be diffracted. The diffracted waves have different transmission directions, which means that the energy is coupled to other modes. This kind of influence is defined as *mode coupling*.

B. In-Mode Loss

The eigenfunction of the propagation mode gives the energy distribution pattern in the tunnel cross section. The energy reflected back by the vehicle's front surface can be obtained using the eigenfunctions. The in-mode loss is the ratio of the energy reflected back to the total energy in the cross section:

$$L_{mn} = \frac{\int_{x_v-\frac{w}{2}}^{x_v+\frac{w}{2}} \int_{-b}^{-b+h} [E^{eign}_{mn,(x,y)}]^2 dxdy}{\int_{-a}^{a}\int_{-b}^{b} [E^{eign}_{mn,(x,y)}]^2 dxdy} \tag{7}$$
$$= \frac{1}{4ab}\left[w - \frac{2a(-1)^m}{m\pi}\cos\left(\frac{m\pi}{a}x_v\right)\sin\left(\frac{m\pi}{a}w\right)\right]\cdot\left[h - \frac{b}{n\pi}\sin\left(\frac{n\pi}{b}h\right)\right].$$

It shows that the in-mode loss is a function of the size and position of the vehicle. Actually, in the section of the tunnel where the vehicle exists, the tunnel cross section in this interval is smaller than the empty tunnel. Additional reflections on the tunnel ceiling and vehicles' roofs are incurred. As a result, the mode attenuation coefficient Γ_{mn} increases. The increased attenuation coefficient causes the additional in-mode loss. However, this part of in-mode loss can be ignored for low order modes, since 1) the low order modes have small grazing angle; 2) the vehicles are sparsely distributed; and 3) the vehicle length is relatively short (less than 20 m).

C. Mode Coupling

The diffraction on the vehicle edges causes a portion of one mode's energy coupling to other modes. The diffraction occurs on the four vertical edges and the two horizontal edges on the vehicle, as shown in Fig. 1.

Proposition 1: In a rectangular tunnel, the vertical edge on an obstruction can only cause one mode to be coupled to the modes that have the same eigenfunctions on y-axes (the eigenfunctions on x-axes can be different). In other words, when mode EH_{mn} is diffracted on a vertical edge, it can only be coupled to the modes $\{EH_{tn}|t = 1, 2, \cdots\}$. Similarly, when mode EH_{mn} is diffracted on a horizontal edge, it can only be coupled to the modes $\{EH_{ms}|s = 1, 2, \cdots\}$.

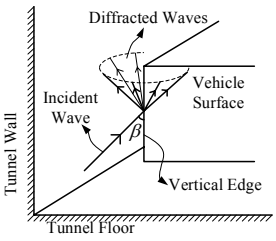

Fig. 2. Diffraction of an incident wave on a vertical edge in the tunnel.

Proof: Here we only prove the vertical edge case. The horizontal edge case can be proved in the same way. Consider that the incident wave of mode EH_{mn} hits a vertical edge, as shown in Fig. 2. The angle between the vertical edge and the direction of the incident wave is β, while the angle between the vertical edge and the direction of the diffracted wave is β'. β is the complementary angle of the grazing angle on the tunnel ceiling/floor β_n ($\beta_n + \beta = 90^\circ$). According to the geometrical theory of diffraction (GTD) [23], β' should be equal to β (forming the *Keller cone*). As a result, the grazing angle of the diffracted waves on the tunnel ceiling/floor is β_n. In the meantime, the diffracted keller cone generates an equivalent radiation source only in the x-z plane. Therefore, after the diffraction on the vertical edge, the mode EH_{mn}'s grazing angle on the vertical walls can change to any value, but the grazing angle on the ceiling/floor remains the same. That is, after diffracted on a vertical edge, mode EH_{mn} can only be coupled to the modes $\{EH_{tn}|t = 1, 2, \cdots\}$. ■

The proposition 1 simplifies the mode coupling analysis in tunnels to two 2-dimensional problems: the mode coupling in x-z plane for the four vertical edges; and the mode coupling in y-z plane for the two horizontal edges. In the following part, detailed calculations of the mode coupling in the y-z plane are given. The results of the mode coupling in the x-z plane can be derived in a similar way. The total mode coupling effect is the superposition of all the six edges' contributions.

Fig. 3 shows the diffracted rays on the two horizontal edges in the y-z plane. The propagation mode EH_{mn} hits the front upper horizontal edge F_0 and the rear upper horizontal edge R_0. Since the attenuation coefficient of the low order mode is small and the vehicle length is usually several meters, the field attenuation and phase shift from the vehicle front to the rear can be ignored. Hence, the fields at the front edge can be considered as the same as the field at the rear edge, which is:

$$\begin{aligned} E^i_{mn} &= C^{Tx}_{mn} \cdot e^{-\Gamma_{mn} z_v} \cdot E^{eign}_{mn,(x,h-b)} \\ &= C^{Tx}_{mn} \cdot e^{-\Gamma_{mn} z_v} \cdot \sin\left(\frac{m\pi}{2a}x + \varphi_x\right) \\ &\quad \cdot \frac{1}{2}\left[\rho_2(n) e^{ik(h-b)\sin(\beta_n)} + \rho_1(n) e^{ik(h-b)\sin(-\beta_n)}\right] \\ &\triangleq E^i_{mn}(\beta_n) + E^i_{mn}(-\beta_n), \end{aligned} \tag{8}$$

where we view the field as the sum of two rays with grazing angle $\pm\beta_n$ on y-z plane.

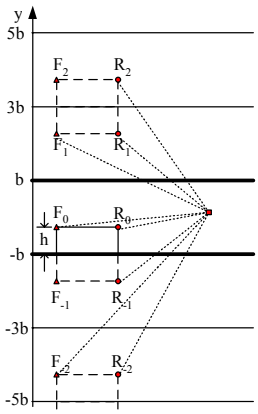

Fig. 3. Side view (y-z plane) of the diffractions on the horizontal edges of a vehicle in the tunnel.

1) Mode Coupling on the Rear Horizontal Edge: We first consider the diffracted field caused by the rear edge. Note that only the incident rays with direction $-\beta_n$ is considered for the diffractions on the rear edge, which is due to the reason that rays with direction β_n cannot hit the rear edge, as shown in Fig. 1(b). The edge can be viewed as a new radiation source. Due to the reflections on the tunnel ceiling/floor, the new source generates periodically positioned source images, as shown in Fig. 3. The diffracted field caused by the rear edge can be calculated by summing up all the rays coming from all the images, which is:

$$E^D(x,y,z+z_v) = \sum_{p=-\infty}^{\infty} E^i_{mn}(-\beta_n)\cdot D(\alpha_m,\pi\mp\phi_p,\beta_n)\cdot R(\phi_p)^{|p|}\cdot\frac{e^{-jkr_p}}{\sqrt{r_p}} \tag{9}$$

where the upper sign is used for the case when p is zero, positive odd or negative even; the lower sign is for other cases; r_p is the distance from image R_p in Fig. 3:

$$r_p = \sqrt{z^2+[2pb\pm(h-b)-y]^2} \qquad \begin{cases} + \text{ if } p \text{ is even} \\ - \text{ if } p \text{ is odd} \end{cases}; \tag{10}$$

ϕ_p is the angle of the grazing angle on the tunnel celing/floor of the rays coming from image R_p; it is also the diffracted angle on the y-z plane:

$$\phi_p = \tan^{-1}\left[\frac{|2pb\pm(h-b)-y|}{z}\right] \qquad \begin{cases} + \text{ if } p \text{ is even} \\ - \text{ if } p \text{ is odd} \end{cases}; \tag{11}$$

$R(\phi_p)$ is the reflection coefficient that can be simplified as an exponential function [3], [4]:

$$R(\phi_p) \simeq -\exp\big(-\frac{2\sin\phi_p}{\sqrt{\varepsilon_w}}\big); \tag{12}$$

$D(\theta_1,\theta_2,\theta_3)$ is the diffraction coefficient on an edge, where $\frac{\pi}{2}-\theta_1$ is the angle between the incident ray and the edge; θ_2 is the angle of the diffracted ray on the plane perpendicular to the edge; and θ_3 is the angle of the incident ray on the plane perpendicular to the edge. Since the GTD method cannot characterize the diffraction near the shadow boundary and the reflection boundary, we use unified theory of diffraction (UTD) to derive the coefficients, which is given in [19, fomula (25)].

To calculate the energy coupled to the other modes, the Poisson summation formula [20] is introduced to translate the sum of rays in (9) to the sum of modes. The ray sum in (9) can be sorted into two parts: the sum of all the functions that the subscript p is even and the sum of the functions that the subscript p is odd:

$$E^D(x,y,z+z_v)=\sum_{q=-\infty}^{\infty} f(4qb+h-b-y)+\sum_{q=-\infty}^{\infty} f(4qd+3b-h-y). \tag{13}$$

Each sum in (13) is a function with period $4b$. According to the Poisson summation formula, the sum of even subscript can be transformed to

$$\sum_{q=-\infty}^{\infty} f(4qb+h-b-y) = \frac{1}{4b}\sum_{s=-\infty}^{\infty} \mathscr{F}_e(s)\cdot e^{j\frac{s\pi}{2b}y}, \tag{14}$$

where the coefficient $\mathscr{F}_e(s)$ is the Fourier transform of the function $f(h-b-y)$ with even subscript:

$$\begin{aligned}\mathscr{F}_e(s) &= \int_{-\infty}^{\infty} f(h-b-y)\cdot e^{-j\frac{s\pi}{2b}y}dy \\ &= E^i_{mn}(-\beta_n)\cdot\int_{-\infty}^{\infty} D(\alpha_m,\pi\mp\phi_0,\beta_n)\cdot(-1)^{p(y)} \\ &\quad\cdot\exp\left(\frac{-2p(y)\sin\phi_0}{\sqrt{\varepsilon_w}}\right)\cdot\frac{e^{-jk\sqrt{z^2+(h-b-y)^2}}}{[z^2+(h-b-y)^2]^{\frac{1}{4}}}\cdot e^{-j\frac{s\pi}{2b}y}\,dy,\end{aligned} \tag{15}$$

where $\phi_0 = \tan^{-1}\left[\frac{|h-b-y|}{z}\right]$. Note that a continuous function $p(y) = |y-h+b|/2b$ is used to approximate the discrete number of reflections on the tunnel ceiling/floor. The motivation for the approximation is to fit the ray sum in (9) to the Poisson sum formula. The saddle-point method [21] is deployed to evaluate the integration in (15). The saddle-point y_{sp} is:

$$y_{sp} \simeq |z|\cdot\tan\beta_s, \tag{16}$$

where β_s is the grazing angle of the mode EH_{ms} on the tunnel ceiling/floor that can be calculated by (6). It is assumed that the order number s is small and the permittivity of the tunnel wall is large. Then, using the saddle point method, we can obtain the approximate result of the integration in (15):

$$\begin{aligned}\mathscr{F}_e(s) &\simeq \frac{1}{2}E^i_{mn}(-\beta_n)\cdot[D(\alpha_m,\pi-|\beta_s|,\beta_n)+D(\alpha_m,\pi+|\beta_s|,\beta_n)] \\ &\quad\cdot\mathrm{sgn}(s)\cdot\frac{\sqrt{2\pi k}}{k\cos(\beta_s)}\cdot e^{-jk\cos(\beta_s)z}\cdot e^{-j\frac{s\pi}{2b}(b-h)}.\end{aligned} \tag{17}$$

The coefficient $\mathscr{F}_o(s)$ for the sum of odd subscript in (13) can be calculated in the same way. Hence the total field right behind the vehicle ($z\simeq 0$) can be expressed as

$$E^D(x,y,0+z_v) = \frac{1}{4b}\sum_{s=-\infty}^{\infty}[\mathscr{F}_e(s)+\mathscr{F}_o(s)]\cdot e^{j\frac{s\pi}{2b}y} \tag{18}$$

$$\begin{aligned}&= \frac{1}{4b}E^i_{mn}(-\beta_n)\sum_{s=1}^{\infty}\big[D(\alpha_m,\pi-\beta_s,\beta_n)+D(\alpha_m,\pi+\beta_s,\beta_n)\big] \\ &\quad\cdot\frac{\sqrt{2\pi k}}{k\cos(\beta_s)}\cdot\cos\left(\frac{s\pi}{2b}h+\varphi_y\right)\cdot\cos\left(\frac{s\pi}{2b}y+\varphi_y\right),\end{aligned}$$

where $\varphi_y = 0$ if s is odd; $\varphi_y = \frac{\pi}{2}$ if s is even. Note that the second line in (18) is exact the sum of the propagation modes.

The total contribution caused by the whole edge can be calculated by integrate (18) along the horizontal edge. Therefore we can derive the coupling coefficient $B^{r,h}_{mn\to ms}$ from mode EH_{mn} to mode EH_{ms} caused by the rear horizontal edge:

$$B^{r,h}_{mn\to ms}=\frac{a\sqrt{2\pi k}\cdot\rho_1(n)}{2m\pi kb\cos(\beta_s)}\cdot e^{ik(h-b)\sin(-\beta_n)}\cdot\cos(\frac{s\pi}{2b}h+\varphi_y) \quad (19)$$
$$\cdot\left[D(\alpha_m,\pi-\beta_s,\beta_n)+D(\alpha_m,\pi+\beta_s,\beta_n)\right]\cdot\sin(\frac{m\pi x_v}{2a}+\varphi_x)\sin(\frac{m\pi w}{4a}),$$

where $\varphi_x=0$ if m is even; $\varphi_x=\frac{\pi}{2}$ if m is odd.

2) Mode Coupling on the Front Horizontal Edge: The mode coupling coefficient for the front horizontal edge can be calculated in the similar way as the rear horizontal edge. As shown in Fig. 3, the only two differences are: 1) the incident waves have both the directions $\pm\beta_n$; and 2) due to the shadow effect of the vehicle itself, not all the images can illuminate the rest of the tunnel; Only the original source, the images with positive odd subscripts and the images with negative subscripts take effects. As a result, the coupling coefficient $B^{f,h}_{mn\to ms}$ from EH_{mn} to EH_{ms} caused by the front horizontal edge can be expressed as

$$B^{f,h}_{mn\to ms}=\frac{a\sqrt{2\pi k}\cdot\sin(\frac{m\pi x_v}{2a}+\varphi_x)\sin(\frac{m\pi w}{4a})\cdot\cos(\frac{s\pi}{2b}h+\varphi_y)}{2m\pi kb\cos(\beta_s)}$$
$$\cdot\left\{\rho_1(n)\cdot e^{ik(h-b)\sin(-\beta_n)}\cdot D(\alpha_m,\pi-\beta_s,\beta_n)\right.$$
$$\left.+\rho_2(n)\cdot e^{ik(h-b)\sin(\beta_n)}\cdot D(\alpha_m,\pi-\beta_s,-\beta_n)\right\}. \quad (20)$$

3) Total Mode Coupling: The mode coupling coefficient for the four vertical edges can be derived in the same way as the horizontal edges. We only need to interchange the x-axes data and the y-axes data. Therefore the total coupling coefficient $B^{total}_{mn\to ms}$ from EH_{mn} to EH_{ms} caused by the vehicle is the sum of the coefficients of the two horizontal edges:

$$B^{total}_{mn\to ms}=\frac{a\sqrt{2\pi k}\cdot\sin(\frac{m\pi x_v}{2a}+\varphi_x)\sin(\frac{m\pi w}{4a})\cdot\cos(\frac{s\pi}{2b}h+\varphi_y)}{2m\pi kb\cos(\beta_s)}$$
$$\cdot\left\{\rho_1(n)\cdot e^{ik(h-b)\sin(-\beta_n)}\cdot\left[2D(\alpha_m,\pi-\beta_s,\beta_n)+D(\alpha_m,\pi+\beta_s,\beta_n)\right]\right.$$
$$\left.+\rho_2(n)\cdot e^{ik(h-b)\sin(\beta_n)}\cdot D(\alpha_m,\pi-\beta_s,-\beta_n)\right\}. \quad (21)$$

The total coupling coefficient $B^{total}_{mn\to tn}$ from EH_{mn} to EH_{tn} caused by the vehicle is the sum of the coefficients of the four vertical edges:

$$B^{total}_{mn\to tn}=(-1)^{\lceil\frac{n}{2}\rceil}\cdot\frac{b\sqrt{2\pi k}}{2n\pi ka\cos(\alpha_t)}\cdot\cos(\frac{n\pi}{2b}h) \quad (22)$$
$$\cdot\left\{\cos(\frac{t\pi}{2a}(x_v+\frac{w}{2}))\cdot\left[\rho_1(m)e^{ik(x_v+\frac{w}{2})\sin(\alpha_m)}\cdot D(\beta_n,\pi-\alpha_t,-\alpha_m)\right.\right.$$
$$\left.+\rho_2(m)e^{ik(x_v+\frac{w}{2})\sin(-\alpha_m)}\cdot\left(2D(\beta_n,\pi-\alpha_t,\alpha_m)+D(\beta_n,\pi+\alpha_t,\alpha_m)\right)\right]$$
$$+\cos(\frac{t\pi}{2a}(x_v-\frac{w}{2}))\cdot\left[\rho_2(m)e^{ik(x_v-\frac{w}{2})\sin(-\alpha_m)}\cdot D(\beta_n,\pi+\alpha_t,\alpha_m)\right.$$
$$\left.\left.+\rho_1(m)e^{ik(x_v-\frac{w}{2})\sin(\alpha_m)}\left(2D(\beta_n,\pi+\alpha_t,-\alpha_m)+D(\beta_n,\pi-\alpha_t,-\alpha_m)\right)\right]\right\}.$$

D. Analytical Expression of a Single Vehicle's Effect

We construct the influence matrix of a vehicle using the results shown in (7), (21) and (22). If there are N significant modes inside the tunnel, the size of the influence matrix $\mathbf{I}$ is $N\times N$. The elements in the diagonal of the matrix consist of the in-mode loss of each significant mode, which is given by (7). The other elements in the matrix are the mode coupling coefficients. According to proposition 1, mode coupling can only happen between two modes that has the same field distribution either in x-z plane or y-z plane. The coupling coefficients between those modes are given by (21) and (22). The mode coupling coefficients between other modes are zero. Given the size and the position of the vehicle, its influence on the signal propagation can be analytically expressed by using the matrix $\mathbf{I}$, which is:

$$\mathbf{I}=\begin{pmatrix}1-L_1 & B^{total}_{2\to1} & \cdots & B^{total}_{N\to1}\\ B^{total}_{1\to2} & 1-L_2 & \cdots & B^{total}_{N\to2}\\ \vdots & \vdots & \ddots & \vdots\\ B^{total}_{1\to N} & B^{total}_{2\to N} & \cdots & 1-L_N\end{pmatrix}. \quad (23)$$

Hence, the intensity of all the significant modes behind a vehicle inside the tunnel are:

$$(C'_1,C'_2,\cdots,C'_N)^T=\mathbf{I}\cdot(C_1,C_2,\cdots,C_N)^T, \quad (24)$$

where $\{C_1,C_2,\ldots,C_N\}$ are the intensity of all the significant modes in front of the vehicle; and $\{C'_1,C'_2,\ldots,C'_N\}$ are the intensity behind the vehicle.

IV. Channel Modeling for Underground Tunnels with Deterministic and Random Vehicular Traffic Flows

In the real tunnels, multiple vehicles exist between the transceivers. In this section, the wireless channels for the L-lane ($L=1,2,...$) road tunnel with deterministic and random vehicular traffic flows are characterized. In particular, we first develop the *deterministic model* for the case when the geometric information of the traffic flow (the size and position of each vehicle) are known. Then we extend the channel model to cover the case when the statistical data of the vehicular traffic flow is given but the exact number, sizes and the positions of the vehicles of the traffic flow between the transceivers are not known. This channel model is defined as *statistical model*. It should be noted that the statistical model is suitable for most real world applications. Finally, the theoretical models are validated by comparing the predicted received power with the simulation results.

A. Deterministic Model

Given the geometric information of the tunnel and all vehicles, the influence of multiple vehicles on the signal propagation can be derived based on the results in Section II and Section III. Assuming that there are M vehicles between the transceivers in the tunnel. The tunnel geometry is the same as Section II. The position and size of the i^{th} vehicle are (x^i_v,z_i) and (w_i,h_i,l_i), respectively. The transmitter is placed in the tunnel cross section where $z=z_0$ and the receiver is placed at (x_r,y_r,z_r). Since the mode propagation can be expressed using matrix [24], [25], the field intensity at the position of the receiver can be expressed as

$$E^{RX}(x_r,y_r,z_r)=\mathbf{E}^{eign}_{(x_r,y_r)}\cdot\mathbf{D}_M\cdot\mathbf{C}^{TX}, \quad (25)$$

where $\mathbf{E}^{eign}_{(x_r,y_r)}$ is the eigenfunction vector at the position (x_r,y_r):

$$\mathbf{E}^{eign}_{(x_r,y_r)}=\left[E^{eign}_{1,(x_r,y_r)},E^{eign}_{2,(x_r,y_r)},\cdots E^{eign}_{N,(x_r,y_r)}\right]; \quad (26)$$

$\mathbf{D}_M$ is the propagation matrix, which is a $N \times N$ matrix that indicates the mode propagation characteristics in the tunnel with M vehicles between the transceivers. $\mathbf{D}_M$ is defined as

$$\mathbf{D}_M = \mathbf{A}(z_r - z_M) \cdot \prod_{i=1}^{M} \left[\mathbf{I}_i \cdot \mathbf{A}(z_i - z_{i-1}) \right], \tag{27}$$

where $\mathbf{A}(z)$ is the mode attenuation matrix for transmitting all the significant modes for z meters in an empty tunnel:

$$\mathbf{A}(z) = \begin{pmatrix} e^{-\Gamma_1 \cdot z} & 0 & \cdots & 0 \\ 0 & e^{-\Gamma_2 \cdot z} & \cdots & 0 \\ \vdots & & \ddots & \vdots \\ 0 & 0 & \cdots & e^{-\Gamma_N \cdot z} \end{pmatrix}; \tag{28}$$

$\mathbf{I}_i$ is the influence matrix caused by the i^{th} vehicle that is defined in (23). $\mathbf{C}^{TX}$ is the mode intensity vector excited by the transmitter at z_0:

$$\mathbf{C}^{TX} = \left[C_1^{TX}, C_2^{TX}, \cdots C_N^{TX} \right]^T. \tag{29}$$

B. Statistical Model

In practical applications, the exact sizes and positions of all vehicles cannot be acquired. Consequently, the propagation matrix $\mathbf{D}_M$ in (27) cannot be accurately calculated. Therefore, instead of using the deterministic vehicular traffic information, we adopt the traffic flow theory and the vehicle size distribution model to predict the propagation matrix $\mathbf{D}_M$.

1) Distribution of the Propagation Matrix $\mathbf{D}_M$: According to (23), (27), and (28), the element D_{uv} in the u^{th} row and the v^{th} column of the propagation matrix $\mathbf{D}_M$ is derived as

$$D_{uv} = \sum_{i_1}^{N} \cdots \sum_{i_{M-1}}^{N} \Big\{ I_{1,\{i_1,v\}} \cdot e^{-\Gamma_v \cdot (z_1 - z_0)} \cdot e^{-\Gamma_{i_M} \cdot (z_r - z_M)} \cdot \prod_{l=2}^{M-1} \left[I_{l,\{i_l,i_{l-1}\}} \cdot e^{-\Gamma_{i_{l-1}} \cdot (z_l - z_{l-1})} \right] \cdot I_{M,\{u,i_{M-1}\}} \cdot e^{-\Gamma_{i_{M-1}} \cdot (z_M - z_{M-1})} \Big\}, \tag{30}$$

where $I_{l,\{i_l,i_{l-1}\}}$ is the element in the ${i_l}^{th}$ row and the ${i_{l-1}}^{th}$ column of the influence matrix $\mathbf{I}_l$. Since $I_{l,\{i_l,i_{l-1}\}}$ and Γ_n are complex, D_{uv} is also complex. Hence it can be expressed as

$$D_{uv} = Re(D_{uv}) + j \cdot Im(D_{uv}). \tag{31}$$

For clear expression, we use $\Theta_{i_1,i_2,\ldots i_{M-1}}$ to denote the addends in the summation in (30). Therefore,

$$D_{uv} = \sum_{i_1}^{N} \sum_{i_2}^{N} \cdots \sum_{i_{M-1}}^{N} \Theta_{i_1,i_2,\ldots i_{M-1}}. \tag{32}$$

Since the tunnel is considered to be long, we assume that the total number of vehicles in the traffic flow is correspondingly large. Moreover, the vehicles have random sizes and positions. Thus, $I_{l,\{i_l,i_{l-1}\}}$ and $(z_l - z_{l-1})$ are random variables. Therefore, $Re(D_{uv})$ and $Im(D_{uv})$ can be viewed as the summation of a sufficiently large number of independent random variables, each with finite mean and variance. According to the central limit theorem and the Lindeberg's condition [26], $Re(D_{uv})$ and $Im(D_{uv})$ are approximately normally distributed.

2) Mean and Variance of the Propagation Matrix $\mathbf{D}_M$: To characterize the above normal distributions, we calculate the mean and variance of $Re(D_{uv})$ according to the traffic flow theory and the vehicle size distribution model. The mean and variance of $Im(D_{uv})$ can be derived in the similar way.

In long road tunnels, there is usually no traffic light and the vehicular traffic flow has only one direction (separate tunnels for traffic with different directions). Hence the vehicular traffic flow can be modeled as a Poisson flow [22]. The total number of the vehicles within the distance d is denoted as M. The probability that the number of vehicles $M = m$ is:

$$P(M = m) = \left(\lambda \frac{d}{v} \right)^m \cdot \frac{1}{m!} \cdot e^{-\lambda \frac{d}{v}}, \tag{33}$$

where λ is the average rate of vehicle arrival (vehicles/sec) in the tunnel; and v is the average velocity of the vehicles. The distance between the i^{th} and $(i-1)^{th}$ vehicle $\Delta z = z_i - z_{i-1}$ obeys independent and identical exponential distribution. The probability density function (pdf) is:

$$f(\Delta z) = \lambda \cdot e^{-\lambda \frac{\Delta z}{v}}. \tag{34}$$

Every vehicle runs in one of the L lanes in the tunnel. Hence the x-coordinate of the i^{th} vehicles x_v^i belongs to $\{a(\frac{1+2l}{L} - 1) | l = 0, 1, \ldots L-1\}$. The x-coordinate of the vehicle obeys uniform distribution with the probability $1/L$. The size of the vehicles are also assumed to have the uniform distribution in the size interval defined in (2).

According to the central limit theorem and the Lindeberg's condition [26], the mean and variance of $Re(D_{uv})$ are approximately the summation of the mean and variance of the real part of each addend in (32), respectively. Therefore,

$$\begin{aligned} E\left[Re(D_{uv})\right] &\simeq \sum_{i_1}^{N} \sum_{i_2}^{N} \cdots \sum_{i_{M-1}}^{N} E\left[Re(\Theta_{i_1,i_2,\ldots i_{M-1}})\right] \\ &= Re\left[E\Big(\sum_{i_1}^{N} \sum_{i_2}^{N} \cdots \sum_{i_{M-1}}^{N} \Theta_{i_1,i_2,\ldots i_{M-1}} \Big) \right]; \end{aligned} \tag{35}$$

$$\begin{aligned} \sigma^2[Re(D_{uv})] &\simeq \sum_{i_1}^{N} \sum_{i_2}^{N} \cdots \sum_{i_{M-1}}^{N} \sigma^2\big[Re(\Theta_{i_1,i_2,\ldots i_{M-1}})\big] \\ &= -E^2\left[Re(D_{uv})\right] + \frac{1}{2} E\Big(\sum_{i_1}^{N} \sum_{i_2}^{N} \cdots \sum_{i_{M-1}}^{N} |\Theta_{i_1,i_2,\ldots i_{M-1}}|^2 \Big) \\ &\quad + \frac{1}{2} Re\left[E\Big(\sum_{i_1}^{N} \sum_{i_2}^{N} \cdots \sum_{i_{M-1}}^{N} \Theta_{i_1,i_2,\ldots i_{M-1}}^2 \Big) \right]. \end{aligned} \tag{36}$$

According to (35), the mean of $Re(D_{uv})$ is the real part of the element in the u^{th} row and the v^{th} column of the mean of the propagation matrix $\mathbf{D}_M$. Since the sizes/positions of all vehicles in the vehicular traffic flow can be viewed as independently and identically distributed, the mean of the propagation matrix $\mathbf{D}_M$ can be calculated as

$$\begin{aligned} E(\mathbf{D}_M) &= E\left[E(\mathbf{D}_M | M = m)\right] \\ &= \sum_{m=0}^{\infty} E[\mathbf{A}(\Delta z)] \cdot \Big\{ E(\mathbf{I}) \cdot E[\mathbf{A}(\Delta z)] \Big\}^m \cdot P(M = m), \end{aligned} \tag{37}$$

where $E(\mathbf{I})$ is the mean of the influence matrix that can be calculated according to (2) and (23); $E[\mathbf{A}(\Delta z)]$ is the mean

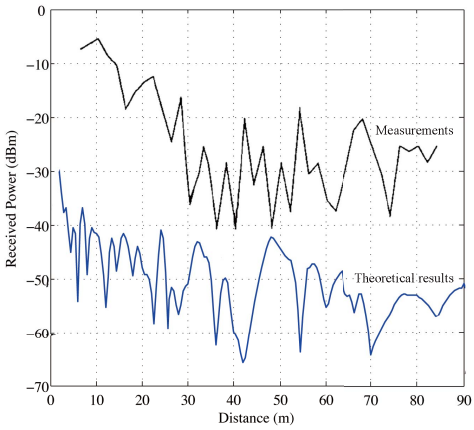

Fig. 4. Received power derived by the experiments and the theoretical models in a straight tunnel with one vehicular 64 m away from the transmitter. For better comparison, the theoretical results are displaced 20 dBm downward.

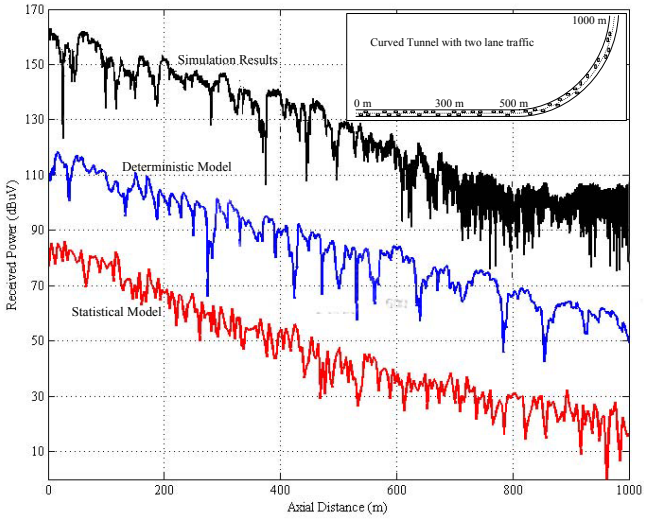

Fig. 5. Received power derived by the simulations and the theoretical models in a curved tunnel with vehicular traffic flow. For better comparison, the simulation results are displaced 40 dBuV upward; and the results calculated by the statistical model are are displaced 40 dBuV downward.

of the mode attenuation matrix that can be calculated using (28) and (34). Based on the Eigendecomposition method [27], the matrix $E(\mathbf{I}) \cdot E[\mathbf{A}(\Delta z)]$ can be decomposed as

$$E(\mathbf{I}) \cdot E[\mathbf{A}(\Delta z)] = \mathbf{V} \cdot \begin{pmatrix} \Lambda_1 & 0 & \cdots & 0 \\ 0 & \Lambda_2 & \cdots & 0 \\ \vdots & \vdots & \ddots & \vdots \\ 0 & 0 & \cdots & \Lambda_N \end{pmatrix} \cdot \mathbf{V}^{-1}, \quad (38)$$

where Λ_i is the i^{th} eigenvalue of the matrix $E(\mathbf{I}) \cdot E[\mathbf{A}(\Delta z)]$; $\mathbf{V}$ is the square $(N \times N)$ matrix whose columns are the eigenvectors of $E(\mathbf{I}) \cdot E[\mathbf{A}(\Delta z)]$. Then, by substituting (33) and (38) into (37), we derive:

$$E(\mathbf{D}_M) \quad (39)$$
$$= \sum_{m=0}^{\infty} \left\{ E[\mathbf{A}(\Delta z)] \cdot \mathbf{V} \cdot \begin{pmatrix} \Lambda_1^m & \cdots & 0 \\ \vdots & \ddots & \vdots \\ 0 & \cdots & \Lambda_N^m \end{pmatrix} \cdot \mathbf{V}^{-1} \cdot \left(\lambda \frac{d}{v}\right)^m \cdot \frac{1}{m!} \cdot e^{-\lambda \frac{d}{v}} \right\}$$
$$= E[\mathbf{A}(\Delta z)] \cdot \mathbf{V} \cdot \begin{pmatrix} e^{\lambda \frac{d}{v}(\Lambda_1 - 1)} & \cdots & 0 \\ \vdots & \ddots & \vdots \\ 0 & \cdots & e^{\lambda \frac{d}{v}(\Lambda_N - 1)} \end{pmatrix} \cdot \mathbf{V}^{-1}.$$

$E[Re(D_{uv})]$ is the real part of the element in the u^{th} row and the v^{th} column of the matrix $E(\mathbf{D}_M)$ given in (39). The variance of $Re(D_{uv})$ (i.e. $\sigma^2[Re(D_{uv})]$) can be calculated in the same way according to (36). Due to limited space, the detail deductions are not elaborated here.

The Gaussian-distributed entries in the propagation matrix $\mathbf{D}_M$ can be completely characterized after the mean and the variance are derived. Then the received power at any positions in the tunnel can be analytically predicted by (25).

C. Comparison with Simulation Results

To validate the proposed channel models, we first compare the derived theoretical results with the measurement provided by [8] in a simple scenario, i.e. a straight tunnel with one vehicle. Then we compare our theoretical results with the numerical simulation results provided by [15] in a more complicated scenario, i.e. a curved tunnel with a vehicular traffic flow. The numerical results in [15] are simulated by the geometrical optics (GO) model. Noted that in the complicated scenario, we use the numerical simulation results instead of the experiment measurements due to the following reasons: 1) it is difficult to conduct experiments in the real road tunnels with many running vehicles; 2) most existing experiment results are taken in empty tunnels; 3) although the GO model requires a great amount of detailed input data of the parameters to describe the tunnel environments and the vehicles, which is impossible in practical applications, the accuracy of the GO model has been widely accepted. We choose the simulation results in [15] because the simulation scenario is complicated enough and very similar to the real road tunnel.

In the experiments conducted in [8], a two lane tunnel with a rectangular cross section 4 m high and 7.5 m wide is used. The transceivers are vertical polarized dipoles placed at the center of the tunnel. The operating frequency is 900 MHz. The tunnel is blocked by a truck on one lane 64 m away from the transmitter. Using the same parameters stated above, we can calculate the received power along the tunnel by the deterministic model. As shown in Fig. 4, the received power calculated by the deterministic model is compared with the measurement given in [8, Fig. 6 (a)]. It is shown that the theoretical results accurately match the measurements.

In the simulation in [15], the tunnel is 1000 m long with 2 lanes. The tunnel cross section has an equivalent rectangle (10 m wide and 6 m high) shape. The tunnel can be viewed as straight for the first 500 m. Form 500 m to 1000 m, the tunnel turns left and forms a $\frac{1}{4}$ circular arc. The transmitter is vertical polarized dipoles at the height of 4.4 m with 1 W power at 945 MHz, which is placed near the entrance of the tunnel. The receiver is also vertical polarized and the coordinate in the tunnel cross is $(2.6\text{ m}, -1.5\text{ m})$. There are 23 vans (1.8 m wide, 1.8 m high, and 5 m long) uniformly distributed on the left lane and 24 buses (2.2 m wide, 3 m high, and 10 m long) uniformly distributed on the right lane.

Using the same scenario parameters stated above, we first

calculate the received power along the tunnel by the deterministic model. As shown in Fig. 5, the received power calculated by the deterministic model is compared with the simulation results given in [16, Bild 6.7]. It is shown that the results derived by the deterministic model match the simulation results accurately. Then the accuracy of the statistical model is tested. The statistical model does not require the size and position information of each specific vehicle. According to the scenario parameters stated above, we can derive that the vehicular traffic flow parameter $\frac{\lambda}{v} = 0.047\ \mathrm{m}^{-1}$. Then the received power along the tunnel can be calculated by the statistical model. In Fig. 5, the received power calculated by the statistical model is compared with the simulation results given in [16, Bild 6.7]. The curve of the statistical model accurately match the simulation results, especially when the axial distance is larger than 200 m. The prediction of the statistical model is less accuracy in the very near region, since the condition of the central limit theorem is no longer valid if the distance between the transceivers is too short. It should be noted that In the curved tunnel section, the prediction accuracy of both the deterministic model and the statistical model is not as high as in the straight tunnel section, which is because that the Eigenfunction in the curved tunnel deviates from its original value. However, the error is small and tolerable.

V. Analysis on Signal Propagation in Tunnels with Vehicular Traffic Flow

In this section, we utilize the proposed channel models to analyze the signal propagations in different tunnels with different vehicular traffic flows. First, we use the deterministic model to analyze the effects of the size, number and the positions of the vehicles on the signal propagation in the tunnels. Then, the statistical model is utilized to give the received power as a function of the transmission distance, vehicular traffic load and vehicle average velocity.

Except studying the effect of certain parameters, default values are set as follows: The tunnel cross section shape is a rectangle with a height of 6 m and a width of 10 m for two-lane tunnels and with a height of 5 m and a width of 6 m for one-lane tunnels; the tunnel wall, ceiling and floor are made of the same material with electrical parameter $\varepsilon_w = 5\varepsilon_0$, $\sigma = 0.01\ S/m$; the tunnel interior is filled with air ($\varepsilon = \varepsilon_0$, $\sigma = 0\ S/m$). The transmitting and receiving antennas are vertically polarized dipoles at the same height (one-third of the tunnel height). Both antennas are placed at the same horizontal position of one-quarter of the tunnel width. The transmitting antenna has the power of 1 W and the impedance of 50 Ω. The operating frequency is 1 GHz.

A. Tunnels with Deterministic Vehicular Traffic Flow

1) Straight One-Lane Road Tunnel: Fig. 6(a) illustrates the effects of the size, number and position of the vehicles on the received power in a straight one-lane tunnel. Compare with the signal propagation in empty tunnels, the existence of the vehicles causes the two impacts: the additional path loss and additional signal fluctuation. These effects can be clearly explained by the theory proposed in Section III: 1) the additional path loss is caused by the in-mode loss; and

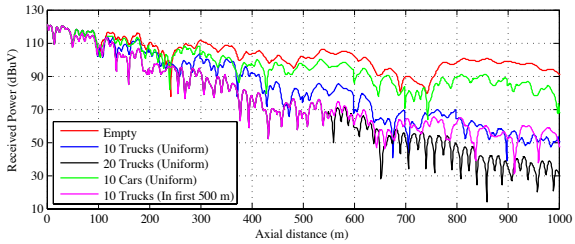

(a) Signal power in straight one-lane road tunnel.

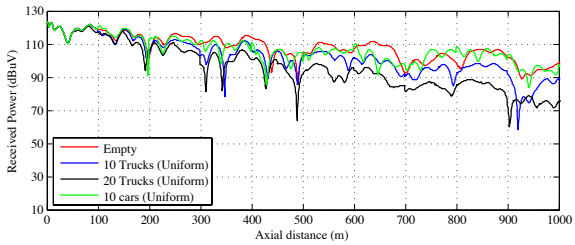

(b) Signal power in straight two-lane road tunnel.

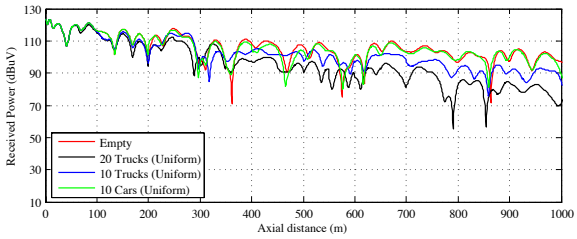

(c) Signal power in curved two-lane road tunnel.

Fig. 6. Signal propagation in tunnels with determined vehicular traffic flows.

2) due to the mode coupling, more significant modes appear behind the vehicle; hence the received signal experiences more serious fluctuations. Comparing the received power when there are 10 trucks with the power when there are 20 trucks, we find that the additional loss and fluctuation are approximately proportional to the number of vehicles. The size of the vehicle has significant effects on the path loss, since the influence of 10 cars is much smaller than the influence of the 10 trucks. We compare the received power when 10 truck are uniformly placed in the 1000 m tunnel and the power when all the trucks are placed in the first 500 m of the tunnel. It indicates that the influence of the axial position of the vehicles is not significant.

2) Straight Two-Lane Road Tunnel: Fig 6(b) shows that the signal propagation in a straight two-lane road tunnel. It shows that the path loss and signal fluctuation are much smaller than the one-lane tunnel. The phenomenon can be explained by the following reasons: 1) the two-lane tunnel has a larger cross section. Hence the signal attenuation of each mode in the empty tunnel is smaller than the one-lane case. 2) the ratio of the vehicle's cross section area to the tunnel's cross section area is much smaller than the one-lane case, hence the in-mode loss and the mode coupling become less significant.

3) Curved Two-Lane Road Tunnel: Fig. 6(c) illustrates the signal propagations in a curved tunnel with different types of vehicular traffic flows. The curve radius of the tunnel is 500 m. Since the attenuation rate of the signal excited by a vertically polarized antenna does not change significantly in the curved tunnels [12], the signal propagation characteristics are similar to the straight tunnel case.

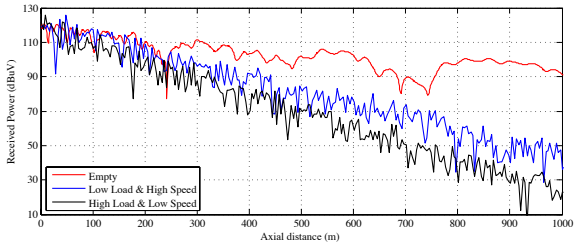

(a) Signal power in straight one-lane road tunnel.

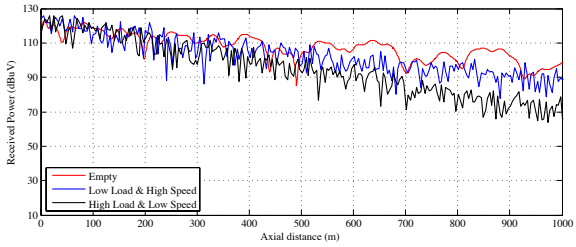

(b) Signal power in straight two-lane road tunnel.

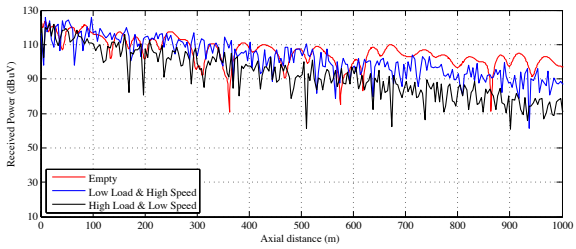

(c) Signal power in curved two-lane road tunnel.

Fig. 7. Signal propagation in tunnels with random vehicular traffic flows

B. Tunnels with Random Vehicular Traffic Flow

In practical applications, the sizes and positions of all the vehicles in the traffic flow are not deterministic. However, the traffic load and the average vehicle velocity can be estimated in the tunnel. Then, our statistical model can be utilized to predict the received power in the road tunnel. In this section, the statistical model is used to analyze the effect of traffic load and the average vehicle velocity. The traffic load is described using the average rate of vehicle arrival λ. We define $\lambda = 0.5$ as the high traffic load case and $\lambda = 0.3$ as the low traffic load case. In the same way, we define the average vehicle velocity $v = 54$ km/hour as the high speed case and $v = 36$ km/hour as the low speed case. It should be noted that the Doppler effect is not considered since the velocity of the vehicles is not high. The motivation to define the vehicle velocity is to determine the mean number of vehicles inside the tunnel.

Fig. 7(a), Fig. 7(b) and Fig. 7(c) show the received power under the influence of different types of vehicular traffic flows in a straight one-lane tunnel, a straight two-lane tunnel, and a curved two-lane tunnel, respectively. The curve radius of the curved tunnel is 500 m. The received power is shown as a function of the transmission distance. According to the statistical model, the sizes of the vehicles are uniformly distributed in the size interval defined in (2). Each vehicle runs in one of the L lanes with the same probability. The number of vehicles in the traffic flow is determined by the traffic load and the vehicle velocity. Fig. 7 shows that the impact of the random vehicular traffic flow is similar to the impact of the deterministic traffic flow. Specifically, 1) The additional loss caused by the traffic flow in the one-lane tunnel is much more significant than the additional loss in the two-lane tunnel, since the same vehicle can block higher ratio of the one-lane tunnel cross section than the two-lane tunnel cross section. 2) The traffic flow with lower load and higher speed causes smaller additional loss than the traffic flow with higher load and lower speed does, which can be explained as follows: When the traffic load is light, fewer vehicles enter the tunnel; and when the average vehicle speed is high, the vehicles in the tunnel leave the tunnel more quickly. Consequently, the number of vehicles in the tunnel is smaller. According to the previous discussion on the effects of vehicle number, the additional path loss caused by the traffic flow with lower load and higher speed should be less significant. 3) In the curved tunnel, the influence of the vehicles on the signal propagation is similar to the straight tunnel case due to the vertically polarized antenna. The signal fluctuation is more severe than the straight tunnel case, which is not caused by the vehicles but the tunnel curvature.

VI. Conclusion

The vehicular traffic flow has significant influence on the wireless signal propagation in the confined underground tunnels. To our knowledge, none of the existing tunnel channel models provide an analytical solution that can explicitly describe the influence of the vehicular traffic flow on the signal propagation. In this paper, we first provide an analytical channel model for the tunnel with a deterministic vehicular traffic flow, which can accurately predict the signal propagation and field distribution in the tunnel. Specifically, the propagation modes experience in-mode loss and mode coupling around a vehicle. The UTD method, Poisson sum formula and saddle point method are utilized to calculate the in-mode loss and mode coupling coefficients. Then based on the deterministic model, a statistical model is developed to characterize the signal propagation in a tunnel with random vehicular traffic flow. Instead of using the deterministic vehicular traffic information, the traffic flow theory and the vehicle size distribution model is utilized. The entries in the propagation matrix are theoretically proved to be normally distributed. In addition, the means and variables of the entries are analytically calculated. Based on the proposed channel model, our analysis shows that: the vehicles in tunnels induce additional path losses and signal fluctuations. In the tunnel with deterministic vehicular traffic flow, the number and size of the vehicle, as well as the size of the tunnel determine the intensity of the vehicles' influence. In the tunnel with random vehicular traffic flow, the average vehicle arriving rate, the average vehicle velocity, and the size of the tunnel determine the additional loss and signal fluctuation caused by the vehicular traffic flow.

Acknowledgment

This work is based upon work supported by the US National Science Foundation (NSF) under Grant No. CCF-0728889.

REFERENCES

[1] I. F. Akyildiz, Z. Sun, and M. C. Vuran, "Signal propagation techniques for wireless underground communication networks," *Physical Commun. J.*, vol. 2, no. 3, pp. 167–183, Sep. 2009.

[2] Z. Sun and I. F. Akyildiz, "Influences of vehicles on signal propagation in road tunnels," in *Proc. IEEE ICC*, May 2010.

[3] Z. Sun and I. F. Akyildiz, "Channel modeling and analysis for wireless networks in underground mines and road tunnels," *IEEE Trans. Commun.*, June 2010.

[4] Z. Sun and I. F. Akyildiz, "Channel modeling of wireless networks in tunnels," in *Proc. IEEE GLOBECOM*, Nov. 2008.

[5] C. Cerasoli, "RF propagation in tunnel environments," in *Proc. IEEE Military Commun. Conf.*, vol. 1, pp. 363–369, Nov. 2004.

[6] D. G. Dudley, M. Lienard, S. F. Mahmoud, and P. Degauque, "Wireless propagation in tunnels," *IEEE Antenna Propagation Mag.*, vol. 49, no. 2, pp. 11–26, Apr. 2007.

[7] S. F. Mahmoud and J. R. Wait, "Geometrical optical approach for electromagnetic wave propagation in rectangular mine tunnels," *Radio Science*, vol. 9, no. 12, pp. 1147–1158, Dec. 1974.

[8] Y. Hwang, Y. P. Zhang, and R. G. Kouyoumjian, "Ray-optical prediction of radio-wave propagation characteristics in tunnel environments part 1: theory; part 2: analysis and measurements," *IEEE Trans. Antenna Propagation*, vol. 46, no. 9, pp. 1328–1345, Sep. 1998.

[9] A. G. Emslie, R. L. Lagace, and P. F. Strong, "Theory of the propagation of UHF radio waves in coal mine tunnels," *IEEE Trans. Antenna Propagation*, vol. AP-23, no. 2, pp. 192-205, Mar. 1975.

[10] K. D. Laakmann and W. H. Steier, "Waveguides: characteristic modes of hollow rectangular dielectric waveguides," *Appl. Optics*, vol. 15, no. 5, pp. 1334–1340, May 1976.

[11] A. Taflove and S. C. Hagness, *Computational Electrodynamics: The Finite-Difference Time-Domain Method*, 3rd edition. Artech House, 2005.

[12] A. V. Popov and N. Y. Zhu, "Modeling radio wave propagation in tunnels with a vectorial parabolic equation," *IEEE Trans. Antenna Propag.*, vol. 48, no. 9, pp. 1403–1412, Sep. 2000.

[13] Y. Yamaguchi, T. Abe, and T. Sekiguchi, "Radio wave propagation loss in the VHF to microwave region due tovehicles in tunnels," *IEEE Trans. Electromagn. Compat.*, vol. 31, no. 1, pp. 87–91, Feb. 1989.

[14] T. Klemenschits, A. L. Scholtz, and E. Bonek, "Microwave measurements in scaled road tunnels modeling 900 MHz propagationin," in *Proc. IEEE VTC*, May 1993.

[15] AWE Communications, "Entwicklung eines programmpakets fur die berechnung der ausbreitung elektromagnetischer wellen in tunnels," Technical Report. Available: http://www.awe-communications.com/Propagation/Tunnel/pdf/tunnel.pdf

[16] C. H. Chen, C. C. Chiu, S. C. Hung, and C. H. Lin, "BER performance of wireless BPSK communication system in tunnels with and without traffic," *Wireless Personal Commun.*, vol. 30, no. 1, pp. 1–12, July 2004.

[17] M. Lienard, S. Betrencourt, and P. Degauque, "Propagation in road tunnels: a statistical analysis of the field distribution and impact of the traffic," *Annals Telecommun.*, vol. 55, no. 11-12, pp. 623–631, Nov. 2000.

[18] K. Arshad, F. A. Katsriku, and A. Lasebae, "Modelling obstructions in straight and curved rectangular tunnels by finite element approach," *J. Electr. Eng.*, vol. 59, no. 1, pp. 9–13, 2008.

[19] R. G. Kouyoumjian and P. H. Pathak, "A uniform geometrical theory of diffraction for an edge in a perfectly conducting surface," *Proc. IEEE*, vol. 62, no. 11, pp. 1448–1461, Nov. 1974.

[20] H. Y. Yee, L. B. Felsen, and J. B. Keller, "Ray theory of reflection from the open end of awaveguide," *SIAM J. Appl. Math.*, vol. 16, no. 2, pp. 268–300, Mar. 1968.

[21] P. Deift and X. Zhou, "A steepest descent method for oscillatory Riemann-Hilbert problems: asymptotics for the MKdV equation," *Ann. Math.*, vol. 137, no. 2, pp. 295–368, 1993.

[22] D. L. Gerlough and M. J. Huber, *Traffic Flow Theory: A Monograph*. Transportation Research Board, National Research Council, 1975.

[23] V. A. Borovikov and B. Ye. Kinber, *Geometrical Theory of Diffraction*. Institution of Electrical Engineers, 1994.

[24] S. Loyka, "Multiantenna capacities of waveguide and cavity channels," *IEEE Trans. Veh. Technol.*, vol. 54, no. 3, pp. 863-872, May 2005.

[25] Z. Sun and I. F. Akyildiz, "Optimal antenna geometry analysis of MIMO communication systems in underground tunnels," in *Proc. IEEE GLOBECOM*, Nov. 2009.

[26] P. Billingsley, *Probability and Measure*, 3rd edition. John Wiley & Sons, 1995.

[27] G. Strang, *Linear Algebra and Its Applications*, 4th edition. Thomson, Brooks/Cole, 2006.

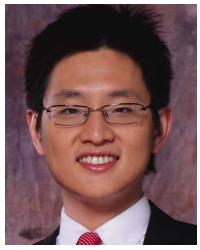

Zhi Sun received B.S. degree in Communication Engineering from Beijing University of Posts and Telecommunications (BUPT), and the M.S. degree in Electronic Engineering from Tsinghua University, Beijing, China, in 2004 and 2007, respectively. He received the Ph.D. degree in Electrical and Computer Engineering from Georgia Institute of Technology, Atlanta, GA. in 2011, under the guidance of Prof. Ian F. Akyildiz. Currently, he is a Postdoctoral Researcher in the Broadband Wireless Networking Laboratory, School of Electrical and Computer Engineering, Georgia Institute of Technology, Atlanta, GA. Dr. Sun received the Best Paper Award in IEEE Globecom 2010. He also received the 2009 Researcher of the Year Award in Broadband Wireless Networking Laboratory, Georgia Institute of Technology and the 2007 Excellent Graduate Student Award in Tsinghua University. His current research interests are in wireless underground networks, wireless sensor networks, and mobile ad hoc networks.

Ian F. Akyildiz received the B.S., M.S., and Ph.D. degrees in Computer Engineering from the University of Erlangen-Nürnberg, Germany, in 1978, 1981 and 1984, respectively. Currently, he is the Ken Byers Chair Professor with the School of Electrical and Computer Engineering, Georgia Institute of Technology, Atlanta, the Director of the Broadband Wireless Networking Laboratory and the Chair of the Telecommunications Group at Georgia Tech. In June 2008, Dr. Akyildiz became an honorary professor with the School of Electrical Engineering at Universitat Politècnica de Catalunya (UPC) in Barcelona, Spain. He is also the Director of the newly founded N3Cat (NaNoNetworking Center in Catalunya). He is also an Honorary Professor with University of Pretoria, South Africa, since March 2009. He is the Editor-in-Chief of *Computer Networks* (Elsevier) journal, and the founding Editor-in-Chief of the *Ad Hoc Networks* (Elsevier) journal, the *Physical Communication* (Elsevier) journal and the *Nano Communication Networks* (Elsevier) journal. Dr. Akyildiz serves on the advisory boards of several research centers, journals, conferences and publication companies. He is an IEEE FELLOW (1996) and an ACM Fellow (1997). He received numerous awards from IEEE and ACM. His research interests are in wireless sensor networks, cognitive radio networks, and nanonetworks.